Appl. Phys. B 68, 989–993 (1999) / DOI 10.1007/s003409900009

Applied Physics B
Lasers
and Optics

Light-induced damage mechanisms in α-phase proton-exchanged $LiNbO_3$ waveguides

A. Alcázar de V.[1], **J. Rams**[2,*], **J.M. Cabrera**[2], **F. Agulló-López**[2]

[1] Depto. Aerotecnia, EUIT Aeronáutica, Universidad Politécnica de Madrid, Plaza del Cardenal Cisneros, 3, E - 28040, Madrid, Spain
[2] Depto. Física de Materiales C-IV, Universidad Autónoma de Madrid, Canto Blanco, E - 28049 Madrid, Spain

Received: 18 November 1998/Revised version: 13 January 1999/Published online: 12 April 1999

Abstract. The overall power and far-field pattern of the beam out-coupled from a single-mode planar proton-exchanged $LiNbO_3$ waveguide in the α-phase have been studied for in-coupled intensities within the range 20–700 W/cm^2. The steady-state output versus input power response shows three definite stages designated as I, II, and III in order of increasing input intensity. In stage I the output varies linearly with input and the far-field pattern does not show appreciable changes. In stage II, the pattern is considerably broadened and displays a number of steady peaks and dips indicative of a filamentary structure of the beam. As in bulk $LiNbO_3$, these damage features are explained in terms of parametric processes involving the amplification of scattered (*noise*) light. An additional broadening is observed in stage III together with the occurrence of a fluctuating profile (chaotic response) attributed to random fluctuations in the coupling parameters. The threshold input intensity separating stages I and II is related to the intensity-dependence of the photovoltaic field.

PACS: 42.82E

Optical waveguides can be prepared on a number of ferroelectric oxide crystals such as $LiNbO_3$, $LiTaO_3$, $BaTiO_3$, $KNbO_3$, and SBN. Fabrication methods are much more advanced for $LiNbO_3$ where commercial integrated optical devices prepared by Ti in-diffusion have been available for more than 15 years [1]. For nonlinear applications, these waveguides suffer from photorefractive damage that rapidly deteriorates the device when it is illuminated with visible light having high or even moderate intensities [2]. Remarkable improvements can be achieved by suitable doping of the $LiNbO_3$ substrate with Mg [3], Zn [4], Sc [5], and In [6] ions. On the other hand, other alternative methods, including ion implantation [7, 8] and proton exchange [9–11] have been more recently developed and show promising possibilities for nonlinear optical (NLO) devices. In particular, proton exchange is a very simple and cheap technique that permits the preparation of a variety of waveguides depending on the fraction x of protons substituting for Li. For $0.01 < x < 0.1$ one obtains the α-phase that presents the same crystalline structure as that of $LiNbO_3$ and so maintains the excellent nonlinear properties of the bulk material [12–14]. Unfortunately, α-phase guides also present photorefractive damage, although their strength and detailed features differ from those corresponding to Ti in-diffused and ion-implanted samples [15–17]. Many scattered data are reported in the literature and a variety of mechanisms have been invoked by different authors to explain the damage features observed in proton-exchanged guides. The experimental conditions, including the type of guide and fabrication method, are different from work to work and often not well specified. There are a few reports [18–21] that do not take into account the new phase diagram of the $H_xLi_{1-x}NbO_3$ compound [14, 22]. Therefore, new experiments on well-characterized samples and well-defined physical conditions together with meaningful analysis of the data are still required. In fact, recent progress in the understanding of the nonlinear processes operating during beam propagation in photorefractive materials [23–28] should help a well-supported analysis of the data.

The purpose of this paper is to present novel detailed data on the steady-state situation and kinetics of photorefractive damage in $LiNbO_3$ waveguides prepared on congruent substrates by proton exchange in the α-phase without post-exchange annealing. Since the structure of α-guides is almost the same as that of bulk $LiNbO_3$, the results can be more meaningfully discussed in terms of mechanisms that have been thoroughly studied in bulk crystals [23–25, 27–29]. In addition to the technological relevance, the damage mechanisms in waveguides have not been sufficiently investigated and offer a wide research area.

1 Experimental methods

A congruent $LiNbO_3$ x-cut wafer, integrated optics grade from Photox Optical Systems (Oxford, UK) was used to prepare a proton-exchanged (α-phase) planar waveguide by immersion in a benzoic acid melt. The melt was buffered with 3% lithium benzoate and the sample was immersed for 24 h at 300 °C within a sealed ampoule. This procedure gives rise to an exchanged layer in the α-phase of better quality

* Present address: Universidad Rey Juan Carlos, ESCET, 28633 Mostoles, Spain

Dedicated to Prof. Dr. Eckard Krätzig on the occasion of his 60th birthday.

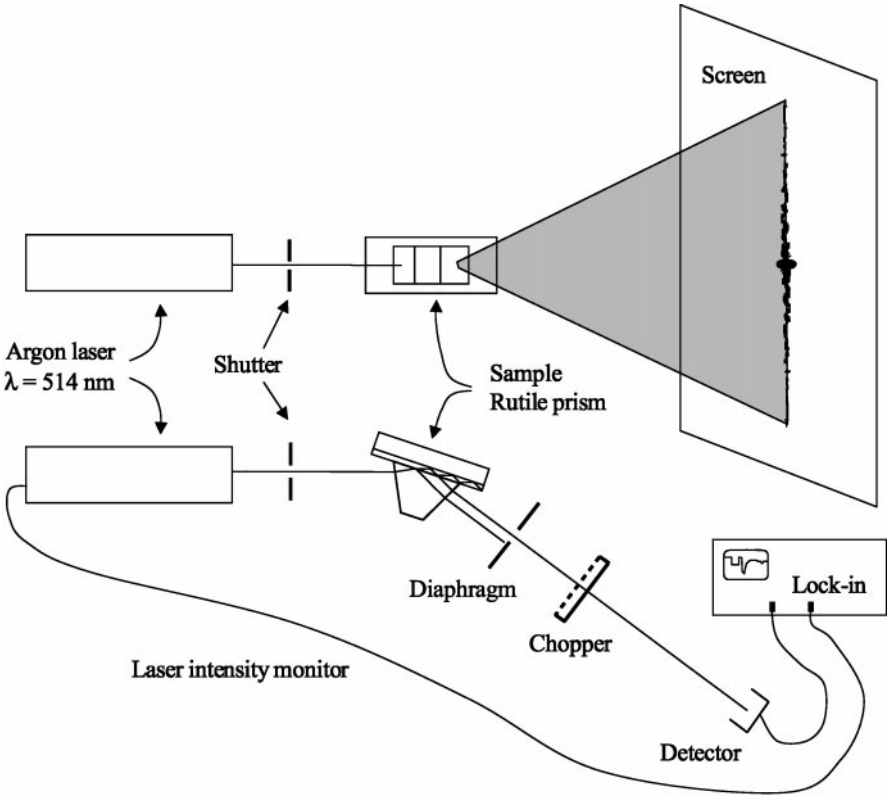

Fig. 1. Experimental setup for observing single-beam photorefractive effects in planar waveguides

than the more popular method of annealing a guide previously prepared in the β-phase [30–32]. A light beam at 514 nm from a 130 mW argon laser was coupled in and out through a rutile prism with appropriated optical contacts separated a distance of 8 mm. The contact area was estimated to be around 1 mm in size. At that wavelength the guide showed a single mode with the electric field along the z axis in the plane of the waveguide (TE mode). The temperature of the sample and sample holder was maintained constant at (30 ± 0.2)°C with a resistance heater and an electronic controller.

Far-field intensity distributions were taken with a vidicon camera (Hamamatsu C-2400-03) with a spectral range of 400–1800 nm and a linearizing control unit (see Fig. 1). The image is digitized and transferred to a personal computer with the help of a frame grabber (Data Translation DT2851) which provides a resolution of 512×512 pixels with a size of 20×15 μm each. Input–output response as well as temporal evolution of the far-field intensity at a certain point was measured with a silicon detector using a chopper and a lock-in amplifier (SR-DSP 850) to improve the signal-to-noise ratio. The laser power was also monitored through an appropriate lock-in output.

2 Results

2.1 Input–output characteristics of waveguides

The steady-state input–output response for the propagating mode of the α-phase guide is displayed in Fig. 2. The output power density is measured at the center of the far-field output pattern through a diaphragm as described above (see Fig. 1). The values represented in Fig. 2 have already been corrected by the coupling efficiency of the contacts. Thus, input intensity stands for the in-coupled intensity at the entrance contact and output intensity stands for the intensity at the exit contact before out-coupling. Three regions are clearly distinguished on the curve and designated as: I (*linear*), II and III (*nonlinear*). In region I, the output intensity is strictly proportional to the input one, while the beam profile does not show any degradation after illumination for 12 h. Region II starts at a power density of about $100\,\mathrm{W/cm^2}$ and is characterized by a reduced output in relation to the linear case. In other words, the waveguide operates as an optical limiter. Region III has similar features to II but the output power has a chaotic fluctuating level,

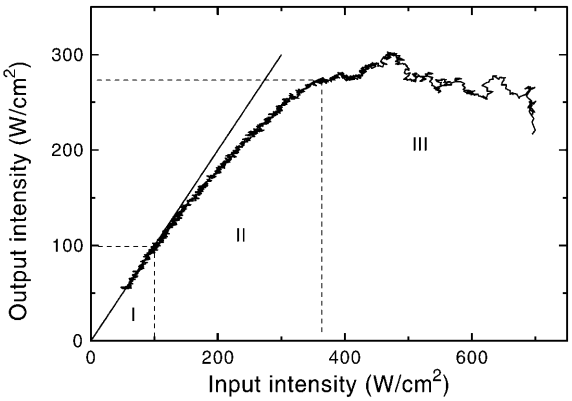

Fig. 2. Output intensity (before out-coupling) versus input intensity (after in-coupling) indicating the three observed regions I, II, and III. The output intensity is measured at the axis of the system

and the internal transmittance is below 50%. The appearance of stage III takes place within the 350–400 W/cm^2 intensity range.

2.2 Far-field patterns

The steady-state far-field patterns, in the vecinity of the beam axis, are shown in Fig. 3, for the three regions of the response curve in Fig. 2. In region I the pattern has a narrow width and the profile is smooth. In region II the width is clearly increased and the profile develops side bumps around the central peak. When examined in detail these bumps appear to display a complex pattern of small peaks and dips that remain stable with time. This structure resembles that found in detailed calculations by Zozulya [26] on bulk $LiNbO_3$, where the propagating beam became striated, i.e. made up of many thin filamentary beams. In region III, the overall beam width further increases and the profile becomes transient and apparently chaotic. The pattern develops a marked asymmetry with a broad shoulder and its angular aperture is about 90°.

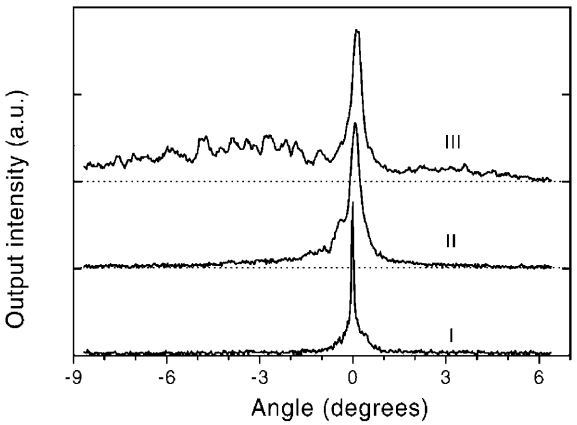

Fig. 3. Far-field intensity profile as measured with the camera for the regions defined in Fig. 2

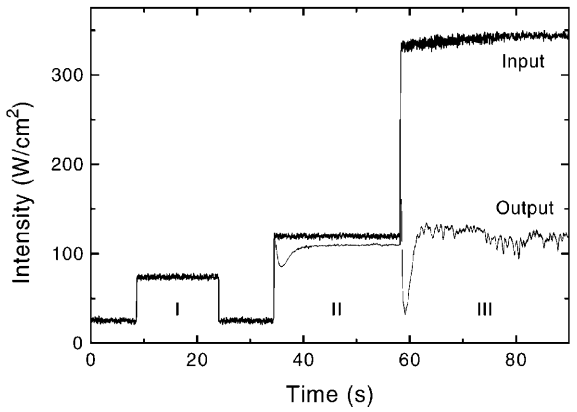

Fig. 4. Kinetics of the output intensity (before out-coupling) when the input intensity (after in-coupling) is suddenly increased from a low value to one corresponding to stages I, II, and III. The *upper curve* corresponds to the input intensity while the *lower* one corresponds to the output intensity taken at the axis of the system

2.3 Kinetics of degradation: transient output

The kinetics of the output intensity when the input intensity is suddenly increased from a low value to one corresponding to stages I, II, and III are shown in Fig. 4. As in Sect. 2.1, the output intensity is measured at the axis of the system through a diaphragm. In addition, all the values represented in the figure correspond to intensities inside the guide, i.e. they have already been corrected for in- and out-coupling efficiencies. In stage I the output power strictly follows the input kinetics. Within the range of powers of stage II, there is first a rapid increase in output up to the level corresponding to the extrapolation of stage I (*linear response*). Then, a decrease is observed in the output due to beam degradation. This decay proceeds down to a minimum and then the output power grows up again to the final steady state. This later growth is indicative of a partial recovery of the induced damage. The same features are observed in stage III, but here the output shows chaotic fluctuations. A complementary behavior is observed if the output power is measured away from the center of the pattern. This indicates that the output power is being transferred from the center to the sides of the far-field pattern.

The transient observed in the output power, measured away from the center at stage II, is illustrated in Fig. 5. Here, the output power increases rapidly after the input power is

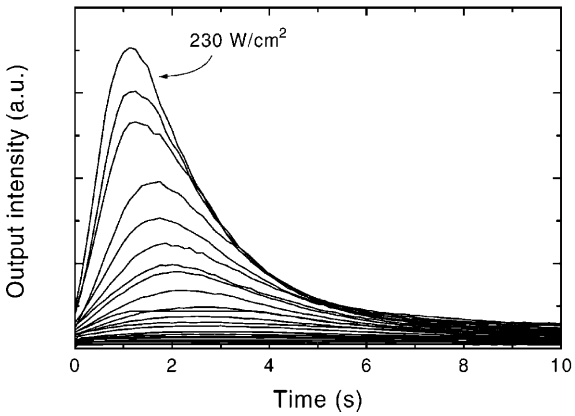

Fig. 5. Kinetics of the output intensity when the input intensity is suddenly increased from a low value to one corresponding to stage II. In this case, the output intensity has been taken away from the axis of the system

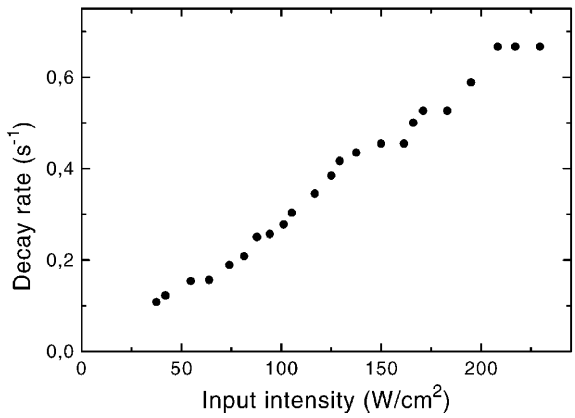

Fig. 6. Decay constant (inverse of the decay time) as a function of the input intensity

set and then decreases down to the final steady-state value. It can be considered as the superimposition of growing and decaying stages whose rates (in the range of s^{-1}) increase with input power. This functional dependence can be more conveniently obtained for the decaying stage, and is illustrated in Fig. 6. It appears that a good linear relation between the decay rate and input power is approximately obeyed.

3 Discussion

A main result of the paper is the appearance of three stages for the beam degradation (*laser damage*) for propagation times up to 12 h. Below an input intensity $\approx 100\,W/cm^2$ (stage I) no appreciable damage is observed. Above this value and up to $\approx 350\,W/cm^2$, the damage monotonically increases with input intensity (stage II). For greater intensities a chaotic damage behavior is observed (stage III). We will next offer a more detailed discussion of our results.

3.1 Stages II and III

The beam degradation observed for high input intensities ($> 100\,W/cm^2$) at regions II and III should be associated to parametric photorefractive processes, i.e. amplification of noise through photorefractive beam coupling. In fact, it presents similar characteristics to those reported for single-beam propagation experiments in bulk crystals. These have been explained by amplification of either the plane-wave components of the beam itself (*photorefractive self-diffraction*) or the light scattered by imperfections (*noise amplification*). It appears now well established that noise amplification is an essential mechanism for the damage [26] and we will consider it in this discussion. Some of these features common to our present waveguide and previous bulk experiments are: (a) broad asymmetric far-field pattern for the output beam, (b) striations in the output intensity profile, and (c) stochastic noise at high input intensities (stage III)

In relation to (a), the shape and evolution of the far-field pattern in our experiments are in good qualitative accordance with the theoretical results of the fanning effect induced by multi-wave mixing and noise amplification as well as experimental results in bulk $BaTiO_3$ [23, 29]. In particular, the angular spread and asymmetry of the pattern is well observed in our waveguide as in previous bulk experiments. Note that the defocusing effects observed in our waveguides are at variance with the strong focusing effects recently reported in SBN for a much smaller spot size [33].

On the other hand, the peak-dip structure of the far-field pattern found in our experiments (feature (b)) closely resembles the profiles found in the experiments and calculations reported by Zozulya [26]. These authors revealed that the fanning of the input beam was made up of many closely packed bright and dark filaments. They arise as a consequence of beam coupling effects between the gratings generated by the different plane-wave components of the incoming beam and noise light.

Finally, stochastic fluctuations in the output beams have been observed in many parametric photorefractive processes at high temperatures. It should be associated with amplification of stochastic space-charge fields possibly generated by random fluctuations in the geometrical parameters, laser intensity, etc. [27]. This should also be the origin of the random fluctuations measured in stage III of our experiments. New and more detailed experiments in this stage III are necessary for a more complete understanding of the involved processes.

The kinetic results illustrated in Fig. 4 can also be qualitatively understood within the proposed parametric amplification model. When the waveguide is suddenly illuminated with a light intensity corresponding to stage III, the output very rapidly tries to reach the level corresponding to the linear (stage I) response. However, as long as the off-axis and noise gratings develop, power is transferred from the central spot of the pattern to the side wings. Consequently a strong decrease is observed in the on-axis light output. The occurrence of the minimum and the subsequent growth of the output intensity may be related to the similar behavior reported in some two- and four-wave mixing experiments [34, 35]. This effect should be reinforced when coupling between multiple gratings is simultaneously taking place.

However, in the case of proton-exchanged waveguides, the explanation may point to thermal (shallow) traps. It has been shown [36] that the competition between optical and thermal traps during photorefractive recording gives rise to peculiar curves showing growth stage up to a maximum followed by a decreasing stage to a steady value. In fact, the relevance of thermal traps on proton-exchanged waveguides has been previously noted [37].

It should be noted that the measured response times after a sudden change in the input intensity are longer than expected from the extrapolation of the values obtained in photorefractive experiments on bulk $LiNbO_3$ [38]. This increase of the relaxation time could be a consequence of the purity of the substrates as well as of the high degree of oxidation of the guides induced by the exchange process. This latter effect has been clearly revealed in experiments on Fe-doped $LiNbO_3$ [39].

3.2 Stage I

It is noticeable that in region I no damage effects have been detected even after exposure times of 12 h. In other words no sign of beam deterioration is observed. However, the input powers are, indeed, sufficient to cause a light-induced change in refractive index (*photorefractive effect*) under the illumination times used in our experiments. In fact, photorefractive gratings are produced and easily measured in bulk $LiNbO_3$ under the same illumination conditions. Moreover, holographic experiments performed in our waveguides have also revealed the generation of measurable refractive index gratings even at power densities of $\lesssim 1\,W/cm^2$. This different behavior is likely associated ta a small photorefractive gain that is not sufficent for amplification of the noise gratings. In these conditions the profile broadening caused by self-diffraction effects cannot be measured in our single-beam experiments. Anyhow, one should be aware of the much higher sensitivity of holographic over single-beam methods.

3.3 Threshold input power

The existence of an input threshold separating stages I and II is a key problem. In principle, it is not consistent with the

simple model for photorefraction. One might take into account the erasing role of the strong dark currents measured in photon-exchange waveguides that may act as a bias to observe photorefractive effects at low light intensities. However, evidence for this effect has not been obtained from the holographic experiments performed in our waveguides. On the other hand, a threshold input power has been found in other parametric amplification processes, suggesting that it may have a rather general origin. A reasonable explanation already advance [40], may be that the photovoltaic field increases at high light intensities and leads to enhanced space-charge fields. Evidences for this effect have been reported for bulk $LiNbO_3$ [41, 42] and waveguides [43]. In particular, the experiments performed on proton-exchange waveguides show marked decreases in the photoconductivity measured at light intensities in the range 100–1000 W/cm^2, i.e. in the same region as our stages II and III.

4 Summary and conclusions

Our experimental results show three well-differentiated stages in the laser damage induced on α-phase proton-exchanged $LiNbO_3$ waveguides. In stage I, observed at low light intensities no appreciable beam degradation is measured and the output and input intensities are proportional. In stages II and III that proportionality is broken and the beam profile is considerably broadened. The effects are similar to those observed in bulk $LiNbO_3$ and should be associated with parametric noise-amplification processes. These enter into a chaotic regime at stage III. The kinetics of damage after a sudden increase in laser intensity show some peculiar features (relatively long response times, bouncing effects) that may be related to particular electronic properties of the exchanged layers.

Acknowledgements. This work was supported by the Spanish Comisión Interministerial para Ciencia y Tecnología under Grant TIC96-0668.

References

1. R.C. Alferness: In *Guided-Wave Optoelectronics*, ed. by T. Tamir (Springer, New York 1988) p. 145
2. V.E. Wood, P.J. Cressman, R.L. Holman, C.M. Verber: In *Photorefractive Materials and Their Applications II*, ed. by P. Günter, J.P. Huignard (Springer, Berlin, Heidelberg 1989) pp. 45–99
3. D.A. Bryan, R. Gerson, H.E. Tomaschke: Appl. Phys. Lett. **44**, 847 (1984)
4. T.R. Volk, V.I. Pryalkin, N.M. Rubinina: Opt. Lett. **15**, 996 (1990)
5. J.K. Yamamoto, K. Kitamura, N. Iyi, S. Kimura, Y. Furukawa, M.S. Sato: Appl. Phys. Lett. **61**, 2156 (1992)
6. T. Volk, M. Wöhlecke, N. Rubinina, N.V. Razumovski, F. Jermann, C. Fisher, R. Böwer: Appl. Phys. A **60**, 217 (1995)
7. P.D. Townsend: Rep. Prog. Phys. **50**(5), 501 (1987)
8. E. Glavas, P.D. Townsend, G. Droungas, M. Dorey, K.K. Wong, L. Allen: Electron. Lett. **23**(2), 73 (1986)
9. J.L. Jackel: Proc. SPIE **1583**, 54 (1991)
10. M.P. de Micheli, D.B. Ostrowski, Yu.N. Korkishko, P. Basi: In *Insulating Materials for Optoelectronics: New Developments*, Ed. F. Agulló-López (World Scientific, London 1995) Chapt. 12
11. J.M. Cabrera, J. Olivares, M. Carrascosa, J. Rams, R. Muller, E. Dieguez: Adv. Phys. **45**, 349 (1996)
12. J. Rams, J. Olivares, J.M. Cabrera: Appl. Phys. Lett. **70**(16), 2026 (1997)
13. J. Rams, J.M. Cabrera: J. Opt. Soc. Am. B, accepted for publication in 1999
14. J. Rams, J.M. Cabrera: J. Appl. Phys. **85**, 1322 (1999)
15. E. Glavas, J.M. Cabrera, P.D. Townsend: J. Phys. D **22**, 611 (1989)
16. T. Fujiwara, R. Srivastava, X. Cao, R. Ramaswamy: Opt. Lett. **18**(5), 346 (1993)
17. A. Alcázar, J. Rams, J.M. Cabrera, F. Agulló-López: J. Appl. Phys. **82**, 4752 (1997)
18. L. Wan, Y. Yuan, G. Assanto: Opt. Commun. **73**, 439 (1989)
19. R. Göring, A. Rasch, W. Karthe: SPIE **1274**, 18 (1990)
20. T. Fujiwara, X. Cao, R. Srivastava, R. Ramaswamy: Appl. Phys. Lett. **61**(7), 743 (1992)
21. Y. Kondo, S. Miyaguchi, A. Onoe, Y. Fujii: Appl. Opt. **33**(16), 3348 (1994)
22. Yu.N. Korkishko, V.A. Fedorov, M.P. De Micheli, P. Baldi, K. El Hadi, A. Leycuras: Appl. Opt. **35**, 7056 (1996)
23. M. Segev, Y. Ophir, B. Fischer: Opt. Commun. **77**, 265 (1990)
24. Q. Wang Song, Ch. Zhang, P.J. Talbot: Appl. Opt. **32**, 7266 (1993)
25. J. Liu, P. Banerjee, Q. Wang Song: J. Opt. Soc. Am. B **11**, 1688 (1994)
26. A.A. Zozulya, M. Saffmen, D.Z. Anderson: Phys. Rev. Lett. **73**, 818 (1994)
27. S.G. Odulov, B.I. Sturman, E. Shamonina, K.H. Ringhofer: Opt. Lett. **21**, 854 (1996)
28. S. Bian, J. Frejlich, K. Ringhofer: Phys. Rev. Lett. **78**, 4035 (1997)
29. J. Feinberg: J. Opt. Soc. Am. **72**, 46 (1982)
30. J. Rams, J. Olivares, J.M. Cabrera: Electron. Lett. **33**, 322 (1997)
31. V.A. Ganshin, Yu.N. Korkishko: Opt. Commun. **86**, 523 (1991)
32. M.L. Bortz, L.A. Eyres, M.M. Feyer: Appl. Phys. Lett. **62**(17), 2012 (1993)
33. D. Kip, E. Krätzig, V. Shandarov, P. Moretti: Opt. Lett. **23**, 343 (1998)
34. M. Horowitz, R. Daisy, B. Fischer: J. Opt. Soc. Am. B **9**, 1685 (1992)
35. M. del Pino, J. Limeres, M. Carrascosa: Opt. Commun. **131**, 211 (1996)
36. F. Jariego, F. Agulló-López: Appl. Opt. **30**(32), 4615 (1991)
37. A. Erdmann: Opt. Commun. **93**, 44 (1992)
38. M. Carrascosa, F. Agulló-López: IEEE J. Quantum Electron. **QE-22**, 1369 (1986)
39. J. Olivares, E. Diéguez, F.J. López, J.M. Cabrera: Appl. Phys. Lett. **61**(6), 624 (1992)
40. B.I. Sturman, M. Aguilar, F. Agulló-López, V. Prunen, P.G. Kazanski, D.C. Hanna: Appl. Phys. Lett. **69**, 1349 (1996)
41. B.I. Sturman, V.M. Fridkin: *The Photovoltaic and Photorefractive Effects in Noncentrosymmetric Materials* (Gordon and Breach, Philadelphia, Tokio 1992)
42. O. Althoff, E. Krätzig: SPIE **1273**, Nonlinear Optical Materials **III**, 12 (1990)
43. R. Göring, Z. Yuang-Ling, St. Steinberg: Appl. Phys. A **57**, 97 (1992)